ARTICLE

ACS chemical biology

Functional Cell-Based Screening and Saturation Transfer Double-Difference NMR Have Identified Haplosamate A as a Cannabinoid Receptor Agonist

Alban Pereira[†], Tom A. Pfeifer[‡], Thomas A. Grigliatti[‡,*], and Raymond J. Andersen[†,*]

[†]Departments of Chemistry and Earth & Ocean Sciences, University of British Columbia, 2036 Main Mall, Vancouver, British Columbia, Canada V6T 1Z1 and [‡]Department of Zoology, University of British Columbia, 6270 University Boulevard, Vancouver, British Columbia, Canada V6T 1Z4

ABSTRACT A marine natural product extract library has been screened with a functional cell-based G-protein coupled receptor assay to find compounds capable of binding the human cannabinoid receptors CB1 and CB2. The methanol extract of the marine sponge *Dasychalina fragilis* collected in Papua New Guinea was active in the assay. Bioassay-guided fractionation of the extract identified the phosphorylated sterol sulfate haplosamate A (**1**) as a cannabinoid receptor agonist. The high water solubility of haplosamate A (**1**) allowed exploration of its binding interactions with the human cannabinoid receptors in whole insect cells by means of saturation transfer double-difference NMR spectroscopy. This technique confirmed that haplosamate A (**1**) binds selectively to these receptors.

Hemp, *Cannabis sativa* L., and its derivatives (such as marijuana, hashish and hash oil) have a long history of use for therapeutic, ritual, and recreational purposes. The Chinese used marijuana for the treatment of malaria, constipation, rheumatic pains, absentmindedness, and gynecological disorders as early as 3000 B.C. (*1–4*). Palliative effects of cannabinoids in cancer patients, which include appetite stimulation, inhibition of nausea and emesis associated with chemo- or radiotherapy, pain relief, mood elevation, and relief from insomnia, have been well known since the 1970s (*3, 5*). Numerous studies have suggested that cannabinoids might also directly inhibit cancer growth through a variety of mechanisms, including induction of apoptosis in tumor cells, antiproliferative action, and an antimetastatic effect involving inhibition of angiogenesis and tumor cell migration (*4, 5*).

Quantitative biological evaluation of the ligand/receptor interactions of cannabinoids both *in vivo* and *in vitro* has been limited by their highly lipophilic nature that severely restricts water solubility (*6*). Crystallization of membrane receptor proteins is extremely difficult, and therefore the structure and shape of the cannabinoid receptors are still not fully characterized and there are no crystallographic data showing receptor-bound cannabinoids (*1, 4, 5*).

RESULTS AND DISCUSSION

As part of an ongoing program designed to discover new biologically active secondary metabolites from marine sources, a library of methanol extracts of marine in-

*Corresponding authors, randersn@interchange.ubc.ca, grigliat@zoology.ubc.ca.

Received for review October 28, 2008 and accepted January 7, 2009.

Published online January 28, 2009

10.1021/cb800264k CCC: $40.75

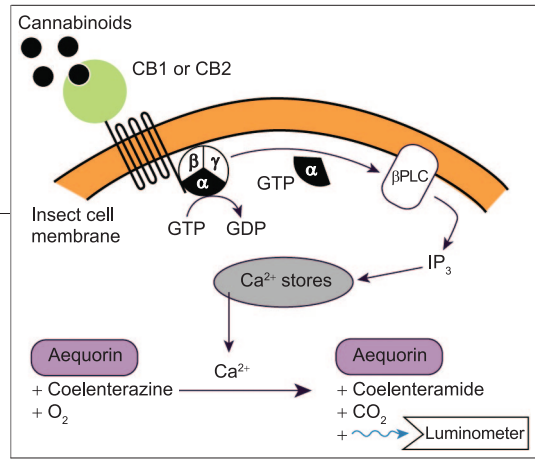

Figure 1. Events involved in the cell-based cannabinoid bioassay (*7*).

vertebrates was screened for cannabinoid activity in a cell-based bioassay. The assay used stable transformed Sf21 (*Spodoptera frugiperda*) cells expressing either one or the other of the human cannabinoid G-protein coupled receptors (GPCRs) CB1 or CB2, along with the human Gα16 G-protein and the Ca^{2+}-sensitive luminescent protein aequorin as a reporter (Figure 1) (*7*). When an agonist binds CB1 or CB2, the signal is transmitted to the insect phospholipase (PLCβ) *via* the human Gα protein, which generates inositol triphosphate (IP3). In the next step, Ca^{2+} is released from intercellular stores *via* an IP3 receptor-mediated response. When Ca^{2+} binds to aequorin, a conformational change takes place that results in the oxidation of bound coelenterazine to coelenteramide with subsequent CO_2 and blue light (λ_{max} 470 nm) production. Since cells do not spontaneously produce light, background noise is extremely low and the emitted blue light is easily detectable with a luminometer (*7*).

A methanol extract of the sponge *Dasychalina fragilis* (Ridley and Dendy, 1886) collected on reefs near Keviang in Papua New Guinea demonstrated strong cannabinoid agonist activity in the assay compared with other marine invertebrate extracts evaluated at the same time. Bioassay-guided fractionation of the *D. fragilis* extract led to the identification of the known phosphorylated sterol sulfate haplosamate A (**1**) (*8, 9*) as the active component in the extract (Scheme 1). The structure of haplosamate A (**1**) was confirmed by comparing its spectroscopic data with literature values (see Supporting Information). An estimate of the EC_{50} for haplosamate A (**1**) in both receptors is ~0.60 mM, which although high is in the same range as the EC_{50}'s for other known agonists such as ACEA (EC_{50} ~0.1 mM for the CB1 receptor) and JWH133 (EC_{50} ~3 mM for CB2) in the assay system. Exposure of **1** to refluxing MeOH containing HCl followed by acetylation of the methanolysis product with acetic anhydride in pyridine gave the triacetate degradation products **2** and **3** (Scheme 1). Acetates **2** and **3** also showed cannabinoid agonist activity in the bioassay with EC_{50}'s comparable to that of haplosamate (**1**), demonstrating that the sulfate and phosphate moieties are not required for CB1 or CB2 receptor binding.

A series of saturation transfer double-difference (STDD) (*10*) NMR experiments were carried out (Figures 2 and 3) to confirm that haplosamate A (**1**) binds selectively to the CB1 and CB2 cannabinoid receptors in whole cells and, at the same time, gain information about which of its structural features directly interact with the receptor proteins. STDD NMR is a technique used to characterize ligand/protein binding interactions at an atomic level, a process often referred to as group epitope mapping (*11–13*). It has been used as

Scheme 1. Assay-guided fractionation of haplosamate A (1) followed by methanolysis to remove the phosphate and sulfate groups and acetylation to generate the triacetates 2 and 3.

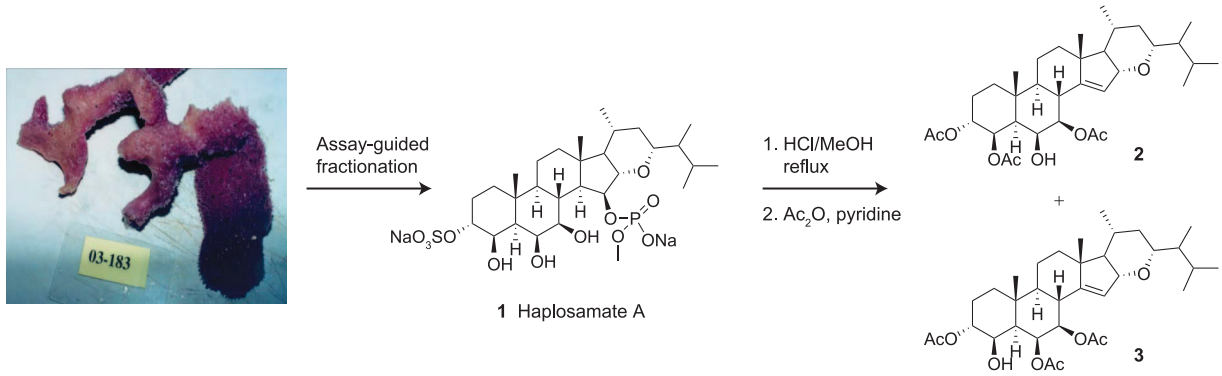

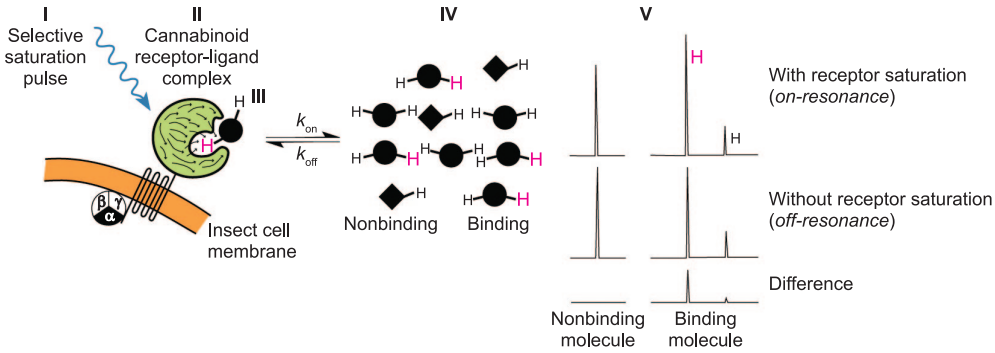

Figure 2. Events involved in saturation transfer difference NMR spectroscopy. (I) Selective saturation of a single protein resonance results in a rapid spread of magnetization over the entire molecule *via* spin diffusion (II). Intermolecular transfer of magnetization from protein to ligand (also by spin diffusion) leads to progressive saturation of the bound ligands (III). This saturation is then transferred into solution through fast exchange of ligand molecules from the bound to the free state (IV), where the saturation-transfer effect is detected. Subtraction of the spectrum without saturation (*off-resonance*) from the one with saturation of the protein (*on-resonance*) yields the final difference spectrum that cancels all resonances, except those from species with binding affinity (V) (*10*).

an efficient tool to study protein−ligand recognition events in a variety of systems (*14*–*18*) for which X-ray analyses of cocrystallized ligand−receptor complexes are not available, making it ideally suited to characterizing the interactions between haplosamate A (**1**) and the CB1 and CB2 receptors.

Figure 3 shows STDD spectra obtained for buffered aqueous solutions of each cannabinoid receptor expressed in Sf21 cells and haplosamate A (**1**) in an approximately 24,000-fold excess of ligand to receptor. The high concentration of sucrose in the media (0.080 mM) generates very intense NMR signals between 3.25−4.25 ppm in the reference spectra (Figure 3, spectra d and f) that cannot be completely subtracted in the STDD spectrum. Therefore, the sucrose resonances show up as a series of dispersion-like peaks in the corresponding STDD spectra and obscure any saturation transfer effects to haplosamate A protons in this region. Signal broadening is a common issue in STDD experiments and results from ligand−receptor exchange processes or fast T_1 relaxation in the protein (*12*). Normally different signal intensities in STDD spectra are best analyzed by integrating the broad proton resonances and referencing them to the most intense signal (*11, 12*). However, the reduced S/R ratio obtained for the STDD spectra in Figure 3 made peak integration impractical in this case.

Two negative controls designed to detect nonspecific interactions that may take place between ligand and host cells were obtained by adding **1** to Sf21 insect cells lacking CB1 and CB2 receptors but containing Gα16 and aequorin and to Sf21 cells expressing retinoschisin (*19*). As shown in Figure 3, spectra a and b, no STDD effects were observed for these control samples, demonstrating that **1** does not bind non-selectively to the cell membranes. In contrast, the STDD spectra in Figure 3 recorded with Sf21 cells containing CB1 and CB2 receptors (spectra c and e) show signals that can be assigned to haplosamate A (**1**). Together, these two sets of data clearly demonstrate that haplosamate (**1**) selectively binds to the human cannabinoid receptors CB1 and CB2 present in the engineered Sf21 insect cells. Often it is possible to identify ligand binding epitopes from STDD spectra since the protons of the ligand that are nearest to the binding site of the protein are expected to be the recipients of the greatest amount of magnetization transfer. The STDD NMR data in Figure 3 show clear saturation transfer effects for all of the resonances assigned to the C-18, C-19, C-21, C-26, C-27, and C-28 methyl groups and the H-6 methine of the steroid nucleus. However, because the poor signal-to-noise ratio in the spectra prevented a satisfactory quantitative analysis, we were not able to use the data to carry out definitive group epitope mapping for the haplosamate A (**1**) binding to the CB1 and CB2 receptors.

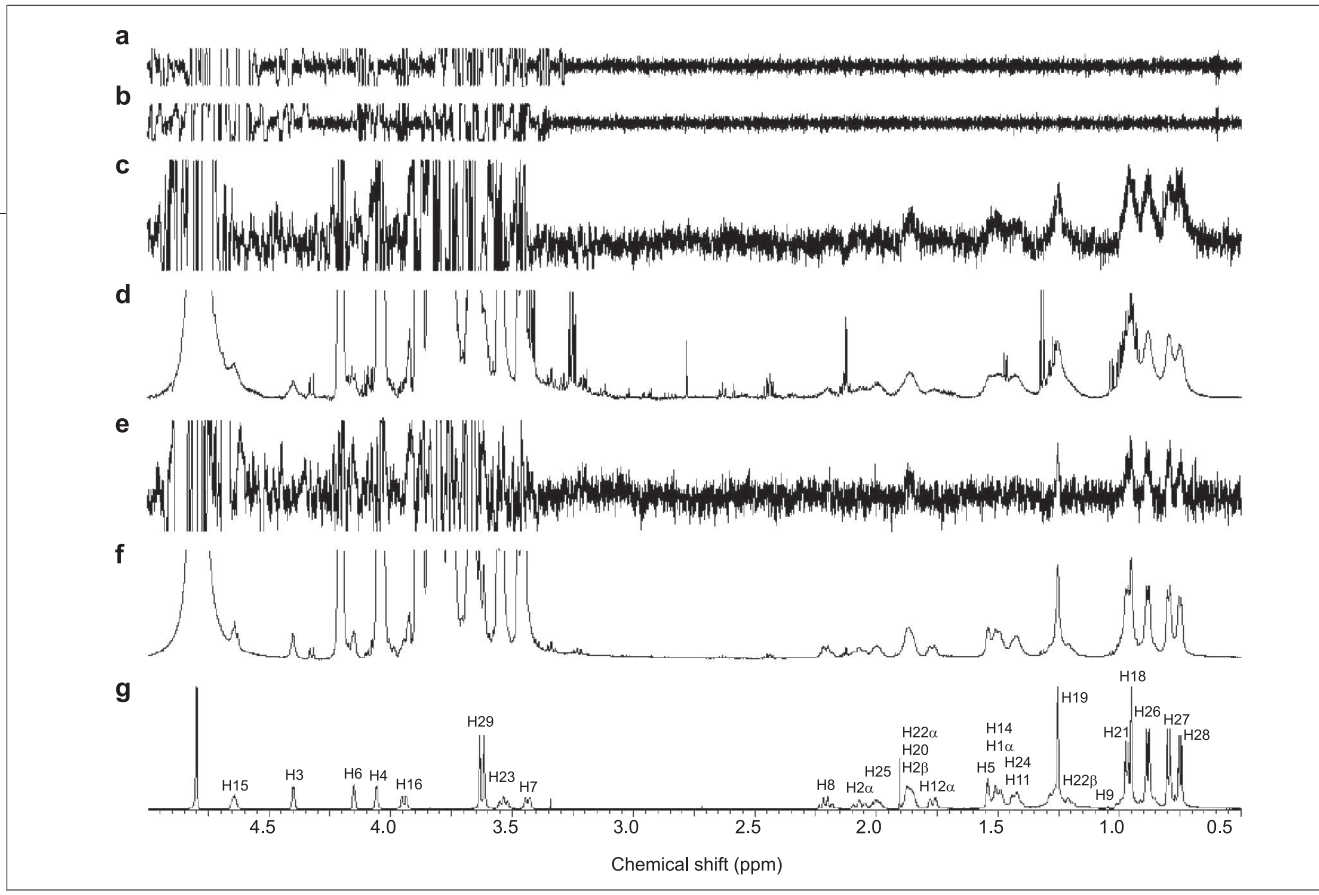

Figure 3. Characterization of the binding interaction between haplosamate A (1) and the human cannabinoid GPCRs CB1 and CB2 in stable transformed Sf21 cells. The media was 11 mM phosphates (pH 6.2), 40 mM NaCl, 40 mM KCl, and 80 mM sucrose in D_2O. (a) STDD spectra of 1 in the presence of Sf21 expressing Gα16 and aequorin and (b) Sf21 cells expressing retinoschisin (*19*), showing that no unspecific binding is present (all resonances for 1 are canceled). (c) STDD spectrum of 1 in the presence of Sf21 cells expressing the CB1 receptor. (d) ^{1}H NMR spectrum of the previous solution given for reference purposes. (e) STDD spectrum of 1 in the presence of Sf21 cells expressing the CB2 receptor. (f) ^{1}H NMR spectrum of the previous solution given for reference purposes. (g) ^{1}H NMR spectrum of 1 (D_2O).

Haplosamate A (**1**) represents a new water-soluble cannabinoid receptor agonist that is not structurally related to any of the known phytocannabinoids, endocannabinoids, or synthetic cannabinoids. The high water solubility of **1** stemming from the presence of sulfate, phosphate, and several hydroxyl groups in its structure has made it possible to explore its binding interactions with the cannabinoid human receptors CB1 and CB2 in whole cells *via* STDD NMR spectroscopy. Crucial to the success of these experiments was the availability of Sf21 cells that either completely lacked cannabinoid receptors or were engineered to express the human CB1 or CB2 receptors. The STDD experiments showed magnetization transfer to haplosamate (**1**) only with cells that expressed CB1 or CB2, demonstrating that the agonist activity exhibited by **1** in the screening assay was the result of selective binding to the cannabinoid receptors. Removal of the phosphate and sulfate groups and acetylation of the alcohol functionalities in **1** did not remove the cannabinoid agonist activity, showing that these functional groups are not required for effective interaction between **1** and the cannabinoid receptors.

Roughly 7% of the human genome codes for transmembrane GPCRs (*13*), such as CB1 and CB2, and many proteins relevant to drug discovery are membrane-bound. It is desirable to study the affinity and specificity of membrane protein interactions with ligands in whole cells. The use of STDD NMR to investigate the interactions between the new water-soluble cannabinoid agonist haplosamate A (**1**) and the cannabinoid receptors CB1 and CB2 in engineered Sf21 cells in the present study represents the first direct evidence of binding between a cannabinoid agonist and a cannabinoid receptor in a whole cell environment.

METHODS

Isolation Procedure. Samples of a red/purple irregular tube sponge (350 g wet wt) were collected by hand using SCUBA at depths of 15 m from reefs off Keviang in Papua New Guinea (2° 45.33′ S, 150° 41.23′ E). The sponge was identified as *Dasychalina fragilis* (Ridley and Dendy, 1886) by R. Van Soest (University of Amsterdam), and a voucher specimen was deposited at the Zoologisch Museum, Amsterdam (ref no. ZMA POR 19111). The collected material was frozen immediately upon collection and transported back to the University of British Co-

lumbia in coolers packed with dry ice. A portion of the frozen material (100 g) was extracted with MeOH (3 × 200 mL), and the combined extracts concentrated to dryness *in vacuo* to give a brown solid (0.60 g). This solid was treated with H_2O to obtain a light yellow solution and an insoluble precipitate. The aqueous layer was extracted sequentially with hexanes (3 × 50 mL), CH_2Cl_2 (3 × 50 mL), and EtOAc (3 × 50 mL), followed by concentration *in vacuo* of each partition. The water-insoluble brown gum (major fraction, 0.38 g) was placed on a small reversed-phase column (20 g) and eluted with MeOH/H_2O (7:3, 200 mL), to afford three major fractions: 183Me1 (0.250 g), 183Me2 (0.032 g), and 183Me3 (0.056 g). 1D and 2D NMR data confirmed the presence of haplosamate A (**1**) in fraction 183Me2, in high purity. Further purification by reversed-phase HPLC using CH_3CN/H_2O (7:3) afforded **1** (0.030 g, 0.043 mmol, 0.008% wet wt) as a white amorphous powder. $[\alpha]^{20}_D$ −5.8 (*c* 0.8, MeOH); UV (MeOH) λ_{max} (log ε) 206 nm (2.98); ^{1}H NMR (CD_3OD, 600 MHz) δ 0.72 (dd, *J* = 10.2, 10.3 Hz, 1H), 0.77 (d, *J* = 7.0 Hz, 3H), 0.82 (d, *J* = 6.8 Hz, 3H), 0.86 (m, 1H), 0.89 (d, *J* = 6.8 Hz, 3H), 0.90 (m, 1H), 0.98 (d, *J* = 6.5 Hz, 3H), 1.00 (s, 3H), 1.20 (td, *J* = 3.9, 12.9 Hz, 1H), 1.32 (s, 3H), 1.33 (m, 2H), 1.40 (m, 1H), 1.43 (m, 1H), 1.45 (m, 1H), 1.50 (m, 1H), 1.52 (m, 1H), 1.64 (d, *J* = 13.4 Hz, 1H), 1.83 (m, 1H), 1.85 (d, *J* = 12.5 Hz, 1H), 1.89 (d, *J* = 14.2 Hz, 1H), 2.07 (m, 1H), 2.09 (m, 1H), 2.30 (dt, *J* = 10.5, 10.6 Hz, 1H), 3.34 (m, 1H), 3.44 (m, 1H), 3.61 (d, *J* = 11.0 Hz, 3H), 3.88 (d, *J* = 9.8 Hz, 1H), 4.01 (s, b, 1H), 4.15 (s, b, 1H), 4.39 (d, *J* = 2.6 Hz, 1H), 4.73 (m, b, 1H); ^{13}C NMR (CD_3OD, 150 MHz) δ 10.8 (CH_3), 15.9 (CH_3), 17.7 (CH_3), 17.9 (CH_3), 20.0 (CH_2), 21.0 (CH_3), 22.0 (CH_3), 23.9 (CH_2), 28.4 (CH), 34.4 (CH), 34.8 (CH), 35.1 (CH_2), 36.7 (C), 40.0 (CH), 41.2 (CH_2), 43.1 (C), 45.3 (CH), 45.6 (CH), 53.4 (d, *J* = 6.0 Hz, CH_3), 54.4 (CH), 58.9 (d, *J* = 7.5 Hz, CH), 63.0 (CH), 76.2 (CH), 77.7 (CH), 78.2 (CH), 80.1 (CH), 82.0 (d, *J* = 7.5 Hz, CH), 82.7 (CH),; 92.4 (CH); ^{31}P NMR (CD_3OD, 81 MHz) δ 0.84 (s, 1P); ESIMS $[M + Na]^+$ calcd for $C_{29}H_{49}O_{12}Na_3PS$ 721.2375, found 721.2377.

Methanolysis of Haplosamate A. A solution of haplosamate A (0.0074 g, 0.0106 mmol) was dissolved in CH_3OH (5 mL) and refluxed for 2 h in the presence of HCl (2 mL, 4 mmol, 2 M). After solvent evaporation, the obtained residue was dissolved in pyridine (2 mL, 24.8 mmol) and treated with acetic anhydride (3 mL, 31.7 mmol). Upon stirring overnight at 25 °C, the solvent was concentrated *in vacuo*, and the resulting solid was purified using normal-phase column chromatography (20 g, EtOAc/hexanes 3:7) to afford two acetylated compounds: triacetate **2** (0.0029 g, 0.0049 mmol, 46%) and triacetate **3** (0.0031 g, 0.0052 mmol, 49%).

Triacetate **2**. ^{1}H NMR (C_6D_6, 600 MHz) δ 0.65 (ddd, *J* = 2.5, 11.9, 11.9 Hz, 1H), 0.87 (d, *J* = 6.6 Hz, 3H), 0.88 (d, *J* = 7.2 Hz, 3H), 0.90 (d, *J* = 6.9 Hz, 3H), 0.90 (s, 3H), 0.94 (d, *J* = 6.9 Hz, 3H), 0.99 (dd, *J* = 1.2, 11.6 Hz, 1H), 1.13 (ddd, *J* = 3.3, 13.6, 14.1 Hz, 1H), 1.16 (ddd, *J* = 3.9, 14.1, 14.6 Hz, 1H), 1.23 (dd, *J* = 8.0, 9.4 Hz, 1H), 1.31 (m, 2H), 1.34 (m, 1H), 1.38 (s, 3H), 1.42 (s, 3H), 1.54 (m, 1H), 1.54 (m, 1H), 1.63 (m, 1H), 1.66 (m, 1H), 1.66 (s, 3H), 1.72 (m, 1H), 1.74 (m, 1H), 1.76 (s, 3H), 1.94 (ddd, *J* = 3.0, 14.4, 14.6Hz, 1H), 2.16 (m, 1H), 2.63 (dd, *J* = 11.3, 11.3 Hz, 1H), 3.38 (m, 1H), 4.13 (dd, *J* = 2.2, 7.1 Hz, 1H), 4.43 (s, broad, 1H), 4.93 (dd, *J* = 3.3, 10.8, 1H), 5.12 (dd, *J* = 1.3, 2.8 Hz, 1H), 5.47 (s, b, 1H), 5.64 (s, b, 1H); ^{13}C NMR (C_6D_6, 150 MHz) δ 11.3 (CH_3), 17.1 (CH_3), 17.9 (CH_3), 18.4 (CH_3), 20.8 (CH_3), 20.9 (CH_3), 21.0 (CH_3), 21.5 (CH_3), 22.0 (CH_2), 22.1 (CH_3), 23.1 (CH_2), 28.2 (CH), 32.0 (CH), 34.8 (CH_2), 36.0 (C), 36.6 (CH), 39.9 (CH_2), 42.3 (CH_2), 44.0 (CH), 44.7 (CH), 46.3 (C), 53.3 (CH), 65.9 (CH), 70.5 (CH), 72.0 (CH), 73.2 (CH), 76.3 (CH), 80.7 (CH), 86.6 (CH), 123.9 (CH), 151.0 (C), 169.2 (C), 169.9 (C), 169.9 (C); ESIMS $[M + Na]^+$ calcd for $C_{34}H_{52}O_8Na$ 611.3560, found 611.3558.

Triacetate **3**. ^{1}H NMR (C_6D_6, 600 MHz) δ 0.68 (ddd, *J* = 2.2, 11.6, 11.6 Hz, 3H), 0.87 (d, *J* = 6.4 Hz, 3H), 0.88 (d, *J* = 6.4 Hz, 3H), 0.89 (d, *J* = 6.4 Hz, 3H), 0.90 (s, 3H), 0.95 (d, *J* = 6.7 Hz, 3H), 0.98 (dd, *J* = 11.6, 12.0 Hz, 1H), 1.11 (ddd, *J* = 3.3, 13.8, 13.8 Hz, 1H), 1.17 (ddd, *J* = 3.3, 13.0, 13.3 Hz, 1H), 1.23 (dd, *J* = 9.7, 10.8 Hz, 1H), 1.31 (m, 1H), 1.31 (m, 1H), 1.33 (s, 3H), 1.40 (m, 1H), 1.42 (m, 1H), 1.54 (m, 1H), 1.54 (m, 1H), 1.62 (m, 1H), 1.66 (m, 1H), 1.67 (s, 3H), 1.72 (s, 3H), 1.73 (dd, *J* = 3.1, 3.6 Hz, 1H), 1.76 (s, 3H), 1.96 (dddd, *J* = 3.1, 3.3, 14.3, 14.4 Hz, 1H), 2.17 (m, 1H), 2.65 (dd, *J* = 11.3, 11.3 Hz, 1H), 3.37 (ddd, *J* = 2.2, 7.2, 9.3 Hz, 1H), 3.51 (m, 1H), 4.12 (dd, *J* = 2.5, 9.4 Hz, 1H), 4.77 (d, *J* = 2.5 Hz, 1H), 5.06 (dd, *J* = 3.8, 11.0, 1H), 5.72 (s, b, 1H), 5.83 (d, *J* = 2.4 Hz, 1H); ^{13}C NMR (C_6D_6, 150 MHz) δ 11.3 (CH_3), 17.1 (CH_3), 18.0 (CH_3), 18.3 (CH_3), 20.8 (CH_3), 21.0 (CH_3), 21.2 (CH_3), 21.4 (CH_3), 21.8 (CH_2), 22.1 (CH_3), 22.2 (CH_2), 28.2 (CH), 32.0 (CH), 35.1 (CH_2), 36.2 (C), 37.2 (CH), 39.4 (CH_2), 42.3 (CH_2), 43.3 (CH), 44.7 (CH), 46.3 (C), 53.3 (CH), 65.8 (CH), 72.6 (CH), 72.8 (CH), 73.3 (CH), 73.8 (CH), 80.7 (CH), 86.5 (CH), 124.3 (CH), 150.7 (C), 169.4 (C), 170.2 (C), 170.6 (C); ESIMS $[M + Na]^+$ calcd for $C_{34}H_{52}O_8Na$ 611.3560, found 611.3564.

STDD NMR Sample Preparation. CB1 or CB2 cell lines were grown to confluency in T75 cell culture flasks and harvested by centrifugation at 500*g*. The cell pellet was resuspended in 10 mL of a deuterated phosphate-buffered modified saline (PMS), prepared in D_2O (99.9%) using 11 mM phosphate (pH 6.2), 40 mM NaCl, 40 mM KCl, and 80 mM sucrose. All preparations were done at RT. The suspension was centrifuged at 500*g* for 10 min, the supernatant was discarded, and the pellet was resuspended in 5 mL of PMS. This wash was repeated two more times, and after the last centrifugation, cell pellets were resuspended in 1.0 mL aliquots of PMS buffer, which provided a cell concentration of approximately 5 × 10^6 cells mL^{-1}. Typical of GPCR-expressing cell lines is a receptor density of about 10^6 per cell, which gives a total concentration of 5 × 10^{13} receptors mL^{-1} (*19*). The NMR samples for each receptor were prepared in pairs of tubes, by previously adding haplosamate A (1.7 mg, 2.0 μmol) to only one NMR tube and splitting the above suspension into both tubes (total volume of each tube, 1.0 mL). This is equivalent to an approximate 24,000-fold excess of ligand to receptor.

STDD NMR Measurements (*10*). STD NMR measurements were made at 298 K with a spectral width of 10 ppm on a 600 MHz spectrometer equipped with a 5 mm inverse double-resonance cryoprobe. Selective protein saturation was achieved by a train of Gaussian pulses of 50 ms length, truncated at 1% and separated by 1 ms delay. Forty selective pulses were applied, leading to a saturation train of 2.04 s. Protein on-resonance irradiation was performed at −1.1 ppm, and the off-resonance irradiation was set at 114 ppm, where no protein signals were present. The number of scans was 64, 256, or 512, preceded by 8 dummy scans. Spectra were subtracted internally by phase cycling after every scan using different memory buffers for on- and off-resonance. A STDD spectrum was obtained by a second manual subtraction of the STD spectrum for [cells + receptor] from the STD spectrum for the [cells + receptor + **1**] sample.

Acknowledgment: We thank N. Burlinson (Chemistry, UBC) for his assistance and useful discussions throughout this work and M. LeBlanc for the collection of the *D. fragilis* specimens. Financial support was provided by NSERC (R.J.A.) and NSERC and CIHR (T.A.G.).

Supporting Information Available: This material is available free of charge *via* the Internet at http://pubs.acs.org.

REFERENCES

1. Felder, C. C., and Glass, M. (1998) Cannabinoid receptors and their endogenous agonists, *Annu. Rev. Pharmacol. Toxicol. 38*, 179–200.

2. Lambert, D. M., and Fowler, C. J. (2005) The endocannabinoid system: drug targets, lead compounds, and potential therapeutic applications, *J. Med. Chem. 48*, 5059–5087.
3. Di Marzo, V., and De Petrocellis, L. (2006) Plant, synthetic, and endogenous cannabinoids in medicine, *Annu. Rev. Med. 57*, 553–574.
4. Pacher, P., Batkai, S., and Kunos, G. (2006) The endocannabinoid system as an emerging target of pharmacotherapy, *Pharmacol. Rev. 58*, 389–462.
5. Guzman, M. (2003) Cannabinoids: potential anticancer agents, *Nat. Rev. Cancer 3*, 745–755.
6. Howlett, A. C., Barth, F., Bonner, T. I., Cabral, G., Casellas, P., Devane, W. A., Felder, C. C., Herkenham, M., Mackie, K., Martin, B. R., Mecholaum, R., and Pertwee, R. G. (2002) International Union of Pharmacology. XXVII. Classification of cannabinoid receptors, *Pharmacol. Rev. 54*, 161–202.
7. Knight, P. J. K., Pfeifer, T. A., and Grigliatti, T. A. (2003) A functional assay for G-protein-coupled receptors using stably transformed insect tissue culture cell lines, *Anal. Biochem. 320*, 88–103.
8. Qureshi, A., and Faulkner, D. J. (1999) Haplosamates A and B: new steroidal sulfamate esters from two haplosclerid sponges, *Tetrahedron 55*, 8323–8330.
9. Fujita, M., Nakao, Y., Matsunaga, S., Seiki, M., Itoh, Y., Soest, R. W. M. V., Heubes, M., Faulkner, D. J., and Fusetani, N. (2001) Isolation and structure elucidation of two phosphorylated sterol sulfates, MT1-MMP inhibitors from a marine sponge *Cribrochalina* sp.: revision of the structures of haplosamates A and B, *Tetrahedron 57*, 3885–3890.
10. Claasen, B., Axmann, M., Meinecke, R., and Meyer, B. (2005) Direct observation of ligand binding to membrane proteins in living cells by a saturation transfer double difference (STDD) NMR spectroscopy method shows a significantly higher affinity of integrin α(IIb)β(3) in native platelets than in liposomes, *J. Am. Chem. Soc. 127*, 916–919.
11. Mayer, M., and Meyer, B. (1999) Characterization of ligand binding by saturation transfer difference NMR spectroscopy, *Angew. Chem., Int. Ed. 38*, 1784–1788.
12. Mayer, M., and Meyer, B. (2001) Group epitope mapping by saturation transfer difference NMR to identify segments of a ligand in direct contact with a protein receptor, *J. Am. Chem. Soc. 123*, 6108–6117.
13. Meinecke, R., and Meyer, B. (2001) Determination of the binding specificity of an integral membrane protein by saturation transfer difference NMR: RGD peptide ligands binding to integrin α(IIb)β(3), *J. Med. Chem. 44*, 3059–3065.
14. Neffe, A. T., Bilang, M., and Meyer, B. (2006) Synthesis and optimization of peptidomimetics as HIV entry inhibitors against the receptor protein CD4 using STD NMR and ligand docking, *Org. Biomol. Chem. 4*, 3259–3267.
15. Murata, T., Hemmi, H., Nakamura, S., Shimizu, K., Suzuki, Y., and Yamaguchi, I. (2005) Structure, epitope mapping, and docking simulation of a gibberellin mimic peptide as a peptidyl mimotope for a hydrophobic ligand, *FEBS J. 272*, 4938–4948.
16. Brecker, L., Straganz, G. D., Tyl, C. E., Steiner, W., and Nidetzky, B. (2006) Saturation-transfer-difference NMR to characterize substrate binding recognition and catalysis of two broadly specific glycoside hydrolases, *J. Mol. Catal. B: Enzym. 42*, 85–89.
17. Milton, M. J., Williamson, R. T., and Koehn, F. E. (2006) Mapping the bound conformation and protein interactions of microtubule destabilizing peptides by STD-NMR spectroscopy, *Bioorg. Med. Chem. Lett. 16*, 4279–4282.
18. Megy, S., Bertho, G., Gharbi-Benarous, J., Baleux, F., Benarous, R., and Girault, J. P. (2006) STD and TRNOESY NMR studies for the epitope mapping of the phosphorylation motif of the oncogenic protein β-catenin recognized by a selective monoclonal antibody, *FEBS Lett. 580*, 5411–5422.
19. Dyka, F. M., Wu, W. W., Pfeifer, T. A., Molday, L. L., Grigliatti, T. A., and Molday, R. S. (2008) Characterization and purification of the discoidin domain-containing protein retinoschisin and its interaction with galactose, *Biochemistry 47*, 9098–10106.